

## Phase transitions of the striped domain-wall phases of S on Ru(0001)

M. Sokolowski\*

*Physikdepartment E20, Technische Universität München, James-Frank-Straße, D-85747 Garching, Germany*

H. Pfnür†

*Institut für Festkörperphysik, Universität Hannover, Appelstraße 2, D-30167 Hannover, Germany*

(Received 21 December 1994)

Atomic sulfur chemisorbed on Ru(0001) forms a striped network of domain walls (DW's) at coverages above completion of a commensurate  $(\sqrt{3} \times \sqrt{3})R30^\circ$  structure ( $\theta > 0.333$ ). At high coverages ( $\theta = 0.48$ ), this DW network transforms into a homogeneous commensurate  $c(2 \times 4)$  structure with an ideal coverage  $\theta = 0.50$ . The temperature-induced phase transitions of the domain walls and the  $c(2 \times 4)$  structure were investigated by low-energy electron diffraction spot profile analysis and compared to theoretical predictions. The phase transition of the superheavy walls, formed at low wall concentrations (coverages  $\theta$  between 0.35 and 0.43), to the disordered lattice gas is found to be continuous, and compatible with a Kosterlitz-Thouless transition expected from theory. At higher coverages light DW's are formed ( $0.43 < \theta < 0.48$ ), which undergo a first-order transition, as evident from an intervening two-phase region formed by the DW phase and the incommensurate phase. Short-range order correlations are maintained in the disordered phase, which is best described by an incommensurate phase with strong disorder. Again a first-order transition is found for the commensurate  $c(2 \times 4)$  structure, which also disorders into a short-range ordered incommensurate phase. Influences by finite-size effects are clearly visible.

### I. INTRODUCTION

Structural phase transitions of adsorbed monolayers on crystal surfaces have gained considerable interest as experimental test systems for two-dimensional (2D) phase transitions during the last years<sup>1-4</sup> as both the phase transitions of commensurate and incommensurate superstructures can be studied. These phase transitions also give access to all types of universality classes in 2D which have a physical realization.

Commensurate structures are typically found for chemisorbed adsorbates at moderate coverages characterized by site-specific adsorption on lattice sites in both the ordered and disordered phases, so that they can be described by lattice gas models. Studies on this type of system are attractive because of their close connection to magnetic models studied extensively in the past,<sup>5</sup> and because of the ease to perform Monte Carlo (MC) simulations on such systems<sup>6</sup> in order to get a deeper understanding of the energy parameters involved by systematically varying them. Experiments performed for a number of different systems have corroborated the theoretical models,<sup>7,8</sup> but have also shown that system-dependent finite-size effects<sup>9</sup> as well as impurities<sup>10</sup> can influence the results considerably, leading to some interesting new physics. In the system under investigation here, both commensurate structures, for which the description just given is adequate, and incommensurate structures together with their phase transitions can be studied. We will focus here on the latter type of structures. Similar to physisorbed systems, particles adsorbed into a completed commensurate structure tend to form domain walls. However, in contrast to physisorbed systems lat-

eral interactions are still small compared with the energy differences of most adsorption sites, so that the classical picture of a relaxation of the whole layer<sup>11</sup> does not seem to be appropriate. Instead the relaxations close to the domain walls (DW's) occur on a length scale of the substrate lattice constant.<sup>12,13</sup>

Nevertheless, the concept of DW's to describe the transition of a commensurate (solid) to an incommensurate (solid) phase and the temperature-induced transition between an incommensurate solid to an incommensurate fluid phase should still be applicable.<sup>11,14</sup> For DW networks with striped symmetry a continuous transition of the Pokrovskii-Talapov-type is predicted for the transition from the commensurate phase to an incommensurate DW phase,<sup>15</sup> whereas a continuous Kosterlitz-Thouless-type transition<sup>16</sup> is expected for the temperature-induced transition from an ordered (solid) DW phase to an incommensurate fluid phase. In contrast, a first-order phase transition due to grain-boundary-induced melting has also been proposed for the latter transition.<sup>17</sup>

Experimentally, DW's with a striped network have been observed both for chemisorbed and physisorbed adsorbates. Examples for chemisorbed systems are H/Fe(110) (Ref. 18), CO/Pt(111) (Ref. 19), and Cs/Cu(110) (Ref. 20), whereas the physisorbed systems Xe/Pt(111) (Ref. 21), H<sub>2</sub>/Gr (Ref. 22), and N<sub>2</sub>/Gr (Ref. 23) should be mentioned. The temperature-induced disordering of the DW's, however, was investigated only in a very small number of systems (see, e.g., Ref. 20).

The aim of the present work was to perform a diffraction study with high resolution on a striped DW system which is well characterized under structural aspects. By means of low-energy electron diffraction (LEED) spot profile analysis we investigated the temperature-driven

phase transitions of striped DW's in the chemisorbed system S/Ru(0001), a surface with hexagonal symmetry, and of the commensurate  $c(2 \times 4)$  structure, which can be viewed as a DW structure with close-packed walls. A change from second to first order is expected as a function of coverage as the phase transition of the  $c(2 \times 4)$  structure should be first order according to the first Landau rule.<sup>5</sup>

The phase diagram, phase transitions, and structure of S/Ru(0001) at different coverages and for different ordered structures have been investigated in some detail in recent years,<sup>8,12,24-29</sup> concentrating on the low-coverage  $p(2 \times 2)$  and  $(\sqrt{3} \times \sqrt{3})R30^\circ$  phases. The adsorption on only the hcp threefold site up to  $\theta = 0.33$  (see Ref. 25), with possible thermally excited occupation of the fcc threefold site<sup>29</sup> at a coverage of 0.33, allows continuous phase transitions for both structures. Both transitions have actually both been observed.<sup>8</sup> Values of critical exponents close to those expected theoretically for the four-state and three-state Potts universality classes<sup>8</sup> have been obtained. Due to the very local bonding characteristics,<sup>12,25,28</sup> phases and phase transitions of this system can be well simulated by lattice gas models.<sup>30,31</sup>

In the present paper, we concentrate on the temperature-driven phase transitions of the DW phases including the  $c(2 \times 4)$  structure. For  $\theta \geq 0.35$ , an ordered striped network of superheavy DW's was found.<sup>24</sup> As evident from both scanning tunnel microscopy<sup>27</sup> (STM) and LEED analysis,<sup>12,13</sup> the walls at low temperature consist of  $c(2 \times 4)$  unit cells with adsorbed S atoms close to both threefold sites. The DW density varies continuously with increasing coverage until the walls are densely packed in the commensurate  $c(2 \times 4)$  structure ( $\theta = 0.48$ ), where both sites are equally populated at  $\theta = 0.50$ . Thus we are left with the unique situation that the domain-wall structure consists of units which are locally fully commensurate [ $(\sqrt{3} \times \sqrt{3})R30^\circ$  and  $c(2 \times 4)$  unit cells], but are combined so that the average is incommensurate.

The paper is organized as follows. After a short description of some experimental details, we report spot profiles showing the formation of DW's and resume the description of structural aspects of the phases at low temperatures from Ref. 24. We then turn to the temperature-driven phase transitions. The results are discussed with respect to experimental results found for other chemisorbed systems and current theories.

## II. EXPERIMENTAL DETAILS

The experiments were performed in a standard UHV chamber (base pressure  $2 \times 10^{-11}$  mbar). Preparation and cleaning of the Ru sample are described in Ref. 8. By LEED profile analysis we found that the prepared surface was oriented  $0.5^\circ$  off the nominal (0001) plane. It consists of terraces with an average width of  $\sim 300$  Å, separated by monoatomic steps.<sup>8</sup>

The sulfur was dosed from an electrochemical cell,<sup>24</sup> and fine-tuning of coverages was done either by temperature-induced partial desorption or by additional

exposure of small amounts of H<sub>2</sub>S.<sup>8</sup> Coverages of sulfur layers were determined from their respective transition temperatures to the disordered phases via the phase diagram which was measured earlier.<sup>24</sup> The transition temperatures were determined from LEED intensity versus temperature curves of the superstructure spots, assigning the transition temperatures to the positions of the inflection points.<sup>32</sup> For the DW structures the coverages could be determined additionally from the spot splitting (see below). Both values agreed within 2%; the latter method was used in the coverage range where splitting in the diffraction patterns could be clearly resolved.

The temperature control of the sample was computerized and had a resolution of 0.1 K.<sup>33</sup> For LEED measurements the direct heating current was chopped with 12.5 Hz, and diffracted electrons were recorded only during off times of the heating current. As temperatures dropped during the measuring intervals, temperatures were effectively averaged over 0.4 K at most.

LEED profile measurements were carried out at a beam energy of 100 eV using a high-resolution LEED instrument (SPALEED).<sup>34</sup> Due to mosaic spread of the sample, the minimal full width at half maximum (FWHM) of LEED spots was limited to a finite value  $\Delta k_{\parallel}$  corresponding to an effective transfer width  $W = 2\pi/\Delta k_{\parallel}$  of 400 Å. This value is below the nominal transfer width of 1200 Å of the SPALEED instrument (for details, see Ref. 8). Further experimental details are described in Refs. 7, 8, and 24.

## III. FORMATION OF DOMAIN WALLS

As we reported in Ref. 24, the diffraction pattern and the observed spot splitting as a function of coverage are only compatible with a network of *superheavy* DW's in a *striped* configuration separating  $\sqrt{3}$  ordered domains.<sup>35</sup> Figure 1(a) shows a hard sphere model of this type of DW's without any lateral relaxation of the walls. In agreement with a recent structural analysis of the  $c(2 \times 4)$  structure,<sup>12</sup> the additional S atoms in the DW's are placed onto fcc sites, whereas only the hcp site is populated in the  $\sqrt{3}$  ordered domains.<sup>25</sup> Locally, the distance between adjacent DW's can take values of

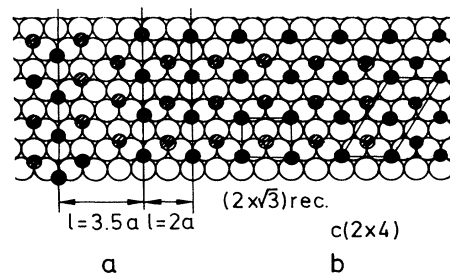


FIG. 1. Hard sphere models for (a) the DW phases with superheavy walls,  $\theta = 0.43$  ( $3/7$ ), and (b) the  $c(2 \times 4)$ - $2S$  structure. The primitive unit cell of the  $c(2 \times 4)$  structure is also indicated. Possible relaxations of atoms from ideal lattice sites are not included.

$(1.5n - 1)a$  with  $n$  being an integer and  $a$  the lattice constant of the substrate. The *average* distance between DW's, however, is not commensurate. For straight DW's without significant meandering the splitting parameter  $\varepsilon$  depends on coverage as<sup>35</sup>

$$\theta = 1/3 \left( 1 + 2\sqrt{3}\varepsilon \right), \quad (1)$$

where  $\varepsilon$  is related to the average DW distance  $l$  by  $l = 1/(2\sqrt{3})a\varepsilon^{-1}$ . Equation (1) was indeed experimentally verified.<sup>24</sup>

A detailed evolution of the spot splitting as a function of coverage is shown in Fig. 2(a) by a series of polar diffraction scans through the first-order  $\sqrt{3}$  superstructure spot (i.e., along the  $\bar{\Gamma}\bar{K}$  direction). The  $\sqrt{3}$  spot splits into six satellites arranged on a triangle around the original  $\sqrt{3}$  spot, as illustrated in Fig. 2(b). They originate from the three rotational domains of the network.

Even with the improved resolution of the experiment carried out here, the lowest coverage at which splitting of the  $\sqrt{3}$  spots and the corresponding formation of an ordered DW network can be detected is again 0.35

[see Fig. 2(a)]. According to Eq. (1), this corresponds to an average distance of the superheavy DW's of  $\sim 60 \text{ \AA}$  or  $23a$ . At these small coverages the spot profiles of the satellites are still broad, due to large fluctuations of the DW distances around the average value of  $l$ , which cause the appearance of the central peak in Fig. 2. With decreasing  $l$  and thus stronger interactions between the walls, the spots become sharper until their width is limited by resolution at  $\theta = 0.38$  ( $l = 22 \text{ \AA}$ ) (see Fig. 2).

The smallest possible value of  $l$  and, therefore, the highest density of superheavy DW's is obtained for  $l = 3.5a$  ( $9.5 \text{ \AA}$ ), i.e., for  $n = 3$ . This is the situation depicted in Fig. 1(a), which corresponds to a coverage of  $\theta = 0.43$  ( $3/7$ ) and leads to the diffraction pattern shown in Fig. 2(b). For the next smaller value of  $n$ , i.e., 2, the  $c(2 \times 4)$  structure [see Fig. 1(b)] is already obtained. This implies that for  $0.43 < \theta < 0.48$  the picture of superheavy DW's is no longer correct. Instead, for  $\theta > 0.43$  a description with light DW's in a  $c(2 \times 4)$  structure is more appropriate. Since the commensurability of the  $c(2 \times 4)$  structure is 4,<sup>36</sup> three different types of light DW's with different local coverages in the walls can be constructed. In Fig. 3 hard sphere models for these three types of DW's are shown. In the DW's the S atoms were placed

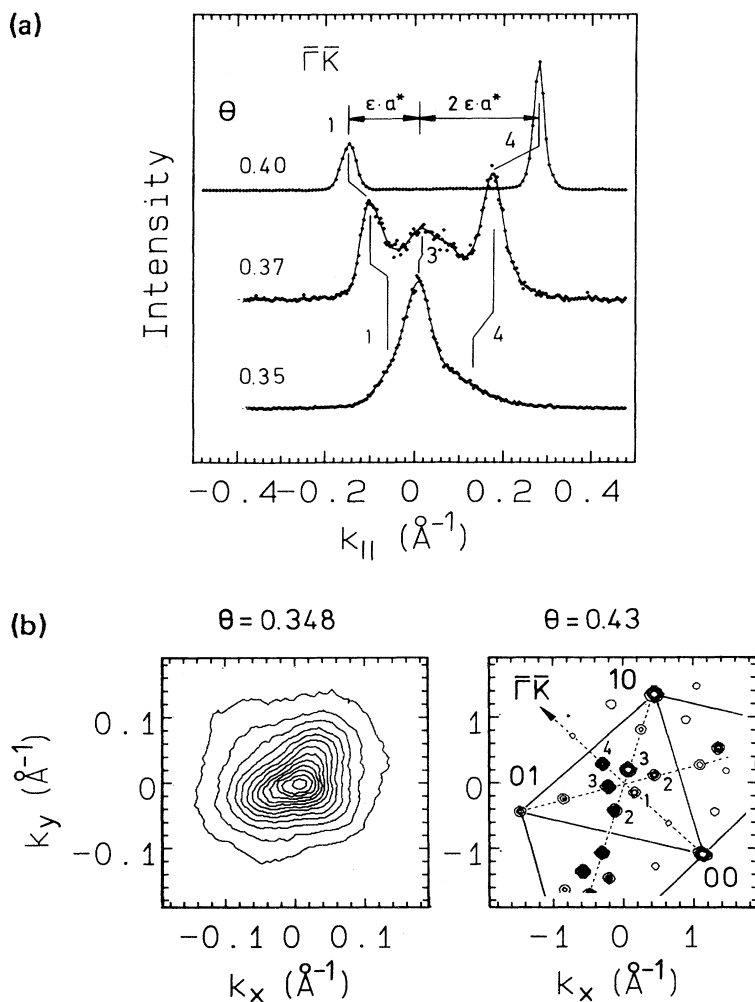


FIG. 2. (a) Evolution of LEED profiles taken along the  $\bar{\Gamma}\bar{K}$  direction through the first-order  $(\sqrt{3} \times \sqrt{3})R30^\circ$  superstructure spot as a function of coverage, illustrating the formation and continuous compression of superheavy DW's for  $\theta \geq 0.35$  in the phase  $E$ .  $k_{||} = 0$  corresponds to the position of the  $(\sqrt{3} \times \sqrt{3})R30^\circ$  superstructure spot. (b) 2D diffraction pattern at  $\theta = 0.35$  and  $0.43$ .  $T = 200 \text{ K}$ . The dashed lines connect spots belonging to one of the three rotational domains of the network.

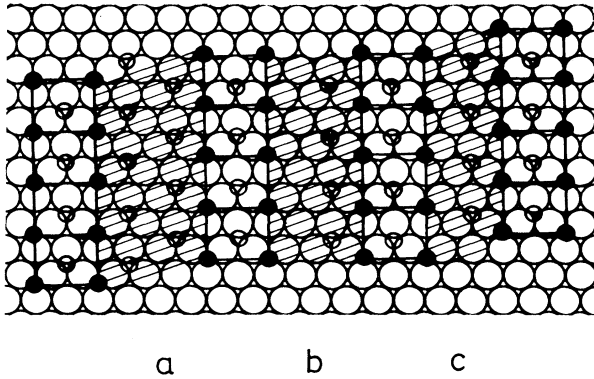


FIG. 3. Hard sphere models for discussed light DW's (hatched areas) in the  $c(2 \times 4)$  structure: (a) light DW's, (b) super-superlight DW's, and (c) super-light DW's. Again, possible relaxations of atoms from ideal lattice sites are not included.

so that the minimal distance between next neighbor S atoms is not smaller than the smallest distance between S atoms in the  $c(2 \times 4)$  structure, since the interaction between the S atoms was found to be repulsive at short distances.<sup>30</sup> From the kinematically constructed diffraction patterns of these models, the relations between  $\theta$  and  $\varepsilon$  are given in Table I. Only models (a) and (c) fulfill Eq. (1). Model (c), however, produces a kinematic diffraction pattern which is at variance with experiment. Light DW's of type (a) also yield the correct structure in the limiting case  $l = 3.5a$ , which has to be identical with that of the superheavy DW's at this wall distance [compare Figs. 1(a) and 3(a)]. Therefore, only light walls of type (a) can exist within domains of the  $c(2 \times 4)$  structure.

The situations at low and high coverages in the domain-wall phase are thus complementary. At  $\theta = 0.35$  a striped network of *superheavy* DW's with  $l = 60 \text{ \AA}$  is formed which is continuously compressed until it transforms into a striped network of *light* DW's at  $\theta = 0.43$ – $0.45$  ( $l = 10$ – $13 \text{ \AA}$ ). With increasing coverage, the density of light walls decreases up to a maximal DW distance of light DW's,  $l = 34 \text{ \AA}$  at  $\theta = 0.48$ .

#### IV. TEMPERATURE-DRIVEN PHASE TRANSITIONS

##### A. Phase transition of the superheavy domain walls

For the analysis of the phase transition of the *superheavy* DW's the peak intensity and the spot profiles of the

most intense of the six satellites [No. 3 in Fig. 2(b)] were measured as a function of temperature. The scan directions of the profiles were chosen perpendicular and parallel to the DW's. The measurements were performed at a coverage of  $\theta = 0.40$ , corresponding to an average DW distance  $l = 14.6 \text{ \AA}$  ( $\varepsilon = 0.054 \pm 0.003$ ). The spot profiles broaden continuously and simultaneously in both scan directions as a function of temperature (see, e.g., Fig. 4), and the peak intensities drop to the background intensity within  $\sim 100 \text{ K}$  above the inflection point ( $T = 298 \pm 5 \text{ K}$ ), as demonstrated in Fig. 5. No shifts of any of the satellites can be detected at the phase transition, and there are no indications for the formation of an ordered phase of different structure.

These observations indicate that the fluctuations of  $l$  increase, while the average value of  $l$  is maintained. Increased fluctuations of  $l$  around a constant average are only feasible if the wall length is extended. As the atom density within the walls is higher than in the  $(\sqrt{3} \times \sqrt{3})R30^\circ$  domains, an increasing amount of material has to be shifted into the walls as a function of temperature, which could be provided by creating point defects within the  $(\sqrt{3} \times \sqrt{3})R30^\circ$  domains. Otherwise, point defects within the walls could provide for the additional wall length or a combination of both processes. The constancy of the average domain-wall separation as a function of temperature is nevertheless remarkable. As the spot intensity of these superstructure spots goes down to the background level at high temperatures, this phase transition is best described by an order-disorder transition to a disordered lattice gas (or fluid), leaving only  $(1 \times 1)$  correlations, most likely with a random occupation of the energetically most favored hcp and fcc sites. Qualitatively, the spot profiles at  $\theta = 0.40$  show very similar variations as a function of temperature as the continuous phase transitions of the  $p(2 \times 2)$  and  $\sqrt{3}$  structures in this system.<sup>8</sup> Therefore, this DW transition is a candidate for a continuous phase transition.

For further analysis of the temperature dependence of the spot profile above  $T_c$ , fits to the data were carried out, using the Ornstein-Zernike approximation of the structure factor<sup>37</sup>

$$S(\mathbf{k}_{\parallel}, t) = \frac{I_0}{(1 + \pi^{-2} \xi_x^2 k_x^2 + \pi^{-2} \xi_y^2 k_y^2)^{1-\eta/2}} * \tau(\mathbf{k}_{\parallel}) + bg(\mathbf{k}_{\parallel}), \quad (2)$$

with  $\mathbf{k}_{\parallel} = (\mathbf{q} - \mathbf{g}_{\parallel})$ .  $\mathbf{q}_{\parallel}$  is the scattering vector, and  $\mathbf{g}_{\parallel}$  the position of the spot in  $k$  space.  $\xi$  denotes the correlation length and  $I_0$  the peak intensity. This parametrization of the structure factor includes two forms of correlation

TABLE I. Possible types of light domain walls in the  $c(2 \times 4)$  structure. Corresponding hard sphere models are shown in Fig. 3. The parameter  $\varepsilon$  denotes the distance of the inner satellites from the position of the commensurate  $(\sqrt{3} \times \sqrt{3})R30^\circ$  spot, in units of  $a^*$ .  $l$  is the average distance between DW's.  $\theta_{\text{DW}}$  denotes the *local* coverage in the DW's.

Type of domain wall	$l/a$	$\theta_{\text{DW}}$	$\theta(\varepsilon)$	$l(\varepsilon)$
a	$2n + 7/2$	$3/7$ (0.43)	$1/3(1 + 2\sqrt{3}\varepsilon)$	$2/3(1 - 4\sqrt{3}\varepsilon)$
b	$2n + 6/2$	$1/3$ (0.33)	$1/6(1 + 2\sqrt{3}\varepsilon)$	$1/3(1 - 4\sqrt{3}\varepsilon)$
c	$2n + 5/2$	$2/5$ (0.40)	$1/3(1 + 2\sqrt{3}\varepsilon)$	$2/9(1 - 4\sqrt{3}\varepsilon)$

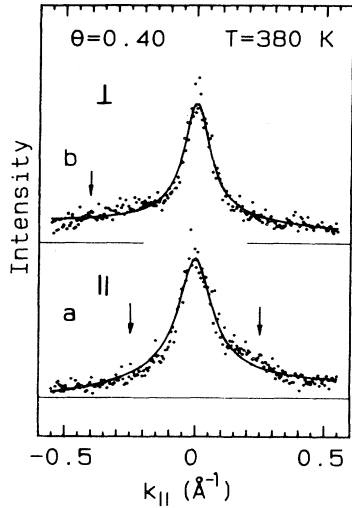


FIG. 4. Phase transition of the superheavy DW's ( $E$ ) to the disordered lattice gas at  $\theta = 0.40$ . Diffraction profiles of the spot No. 3 (see Fig. 2) above the phase transition,  $T = 380$  K, in the directions perpendicular (a) and parallel (b) to the DW's. The solid line represents a fit to the profile according to Eq. (2). The arrows indicate the positions of the neighboring satellites. The zero position of the  $k_{\parallel}$  axis is fixed to the peak maximum.

functions which are generally discussed for DW phase transitions. For  $\xi k_{\parallel} \gg 1$  a power law is obtained for the structure factor  $S(k_{\parallel}) \propto (\xi k_{\parallel})^{-(2-\eta)}$ , which describes an algebraic decay of DW correlations  $\propto r^{-\eta}$  (see Refs. 38, 39). On the other hand, a Lorentzian form is obtained for  $S(k_{\parallel})$ , when  $\eta = 0$ . It describes the case of an exponentially decaying correlation function [ $\propto \exp(-r/\xi)$ ].<sup>40</sup> For continuous order-disorder phase transitions of commensurate phases, this latter form was experimentally found to be a useful parametrization.<sup>7,8</sup>

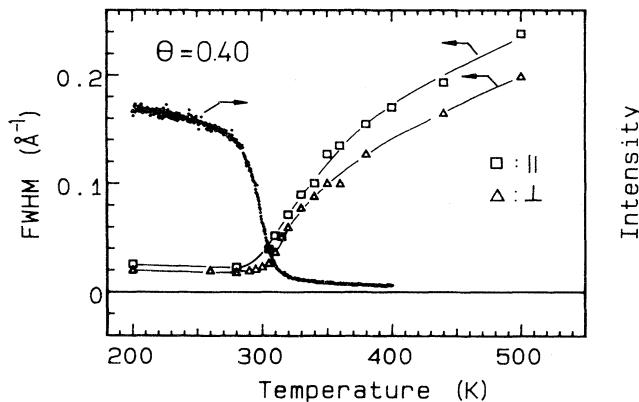


FIG. 5. Phase transition of the superheavy DW phase ( $E$ ) to the disordered lattice gas at  $\theta = 0.40$ . Peak intensity and FWHM of the diffraction spot No. 3 in the directions perpendicular and parallel to the DW's as a function of temperature.

The last term in Eq. (2),  $bg(\mathbf{k}_{\parallel})$ , corresponds to a constant background which was also fitted. The indices  $x$  and  $y$  denote the directions perpendicular and parallel to the DW's, respectively. Fits to the experimental profiles were carried out using Eq. (2) for  $S(k_{\parallel})$ . The numerical procedures imply a 2D convolution with the instrumental profile  $\tau(\mathbf{k}_{\parallel})$  and one-dimensional cuts (along the  $x$  and  $y$  axes) for comparison with experimental profiles. The instrument function was modeled by experimental profiles taken at temperatures far below the phase transition. For further details of the data evaluation, see Refs. 7, 8.

At high temperatures, due to their increased half widths, the profiles from different satellite peaks start to overlap, making the profiles slightly asymmetric. In Fig. 4, the positions of the next neighbor satellites are indicated, and the weak shoulder on the right side of the spot profile shown in Fig. 4(a) is possibly due to this effect. Since the intensity of the neighboring satellites, however, is about a factor of 5 and 2 smaller for directions parallel and perpendicular to the DW's, respectively, we do not expect a significant influence of this overlap on the results of the fits. In particular, the values of the correlation lengths derived from the FWHM should be influenced very little.

Fitted values of  $\xi_{x,y}$  and  $\eta$  are plotted in Fig. 6 versus the reduced temperature  $t = T/T_c - 1$ . The transition temperature  $T_c = 298 \pm 5$  K was assumed to be at the inflection point of the peak intensity versus temperature curve [ $I(T)$  curve]. For continuous phase transitions (with  $\alpha \neq 0$ ), this is strictly correct if the instrument effectively integrates over the fluctuations.<sup>32</sup> If the correlation length is limited by finite-size effects like in the present system, this condition is not fulfilled for our high-resolution instrument, but turned out experimentally to

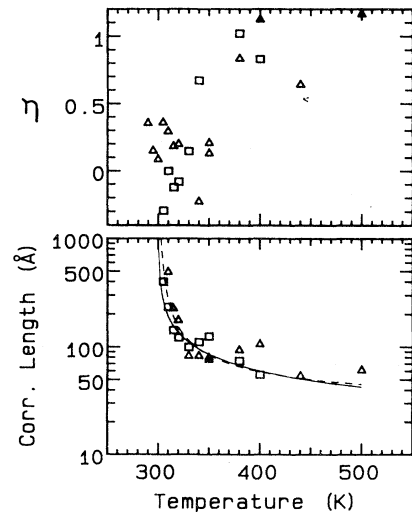


FIG. 6. Phase transition of the superheavy DW phase ( $\theta = 0.40$ ). Fitted exponent  $\eta$  and correlation length as a function of temperature. The dashed line is a fit to the predicted temperature dependence of a KT phase transition; the solid line is a fit to a power law singularity with [Eq. (4)]  $\nu = 0.50$ . For further details see text.

be still valid to a good approximation.<sup>8</sup> For a Kosterlitz-Thouless (KT) phase transition, however, no specific heat anomaly exists. In this case, our determination of  $T_c$  can only be considered as an *ad hoc* definition.

Above the critical temperature, the beam profiles get broader. Within the scatter of the data, the same temperature dependence of the values fitted for  $\xi$  and  $\eta$  is found in the directions perpendicular ( $\perp$ ) and parallel ( $\parallel$ ) to the DW's (see Fig. 6). As seen from this figure, the temperature dependence of the correlation lengths can be described by a power law singularity

$$\xi \propto t^{-\nu}, \quad (3)$$

with a temperature-independent critical exponent  $\nu$ , but also equally well by the form

$$\xi \propto \exp[b(T - T_c)^{-\nu}], \quad (4)$$

characteristic for a KT transition, with  $\nu$  set to 0.396.<sup>38</sup> Using Eq. (3), a value of  $\nu = 0.50$  is estimated. Thus, no clear evidence for a KT phase transition can be obtained from the measured temperature dependence of the correlation lengths.

A criterion, which clearly favors the existence of a KT transition, is the temperature dependence of the exponent  $\eta$ . The determined values of the exponent  $\eta$  (see Fig. 6) are also subject to large uncertainties, especially since only a small range in the variable  $y = \xi k_{\parallel}$  can be fitted here.<sup>8</sup> Nevertheless, the data indicate that  $\eta$  depends on temperature, and increases with  $T$ . This behaviour is expected for a KT transition [ $\eta \propto T$  (Ref. 38)], but would be incompatible with any other kind of continuous order-disorder phase transition with a power law singularity, where  $\eta$  should not depend on temperature.<sup>40</sup> A temperature-independent value of  $\eta$  has been found, e.g., in the order-disorder transition of the  $p(2 \times 2)$  structure of S/Ru(0001), which was shown to belong to the universality class of the four-state Potts model.<sup>8</sup>

Therefore, we conclude that we most likely have found a KT transition at this coverage of 0.40. The main mechanism of a KT transition is the formation of free dislocations.<sup>38</sup> For a striped DW lattice, these dislocations consist of points in the DW network where three DW's merge.<sup>41</sup> The formation of the dislocations has two effects. First, the fluctuation in the DW distance increases, and second, the correlation of the atoms on the  $\sqrt{3}$  lattice along the average direction of the DW's is lost. For this scenario, a common decrease of the correlation lengths in the directions parallel and perpendicular to the average DW direction is expected, and was indeed observed here.

Although the alternative possibility of a first-order phase transition cannot be ruled out right away, it does not seem to be very likely. In this case, the decrease of  $\xi$  would have to be explained by the formation of small islands of the ordered DW structure which are surrounded by a disordered phase. The quasicontinuous behavior would have to be interpreted to be due to finite-size effects. For a first-order transition, however, the transition would be spread out over an extraordinarily large

temperature range, much larger than found for the first-order transition of the  $c(2 \times 4)$  phase at higher coverage described below. The behavior observed here is also fundamentally different from that found at slightly higher coverage in the domain-wall phase described in the next section. A first-order transition would also not explain the observed increase of  $\eta$ . We thus come to the conclusion that the transition is continuous and most likely a KT transition.

## B. Wall-wall transition

An additional phase appears at coverages slightly above the completion of the commensurate  $\sqrt{3}$  structure, i.e., for  $0.334 < \theta < 0.355$ , and at temperatures  $T > 240$  K, termed  $E'$ . At temperatures between 240 and 420 K an increase of coverage above the completed  $\sqrt{3}$  structure leads to isotropic broadening of the  $\sqrt{3}$  spot profiles of about 50%, indicative for the presence of line defects and/or antiphase boundaries in this phase. Upon further increase of coverage or temperature, this phase undergoes an order-disorder phase transition. Lowering the temperature causes a phase transition from  $E'$  to  $E$ , which is indicated by a sudden broadening of spot profiles. For  $\theta = 0.346$ , e.g., this broadening amounts to about 30%. Unfortunately, no more detailed information can be obtained because satellites are not resolvable. However, a further indication of the different nature of the  $E'$  phase compared to  $E$  is provided by the hysteresis effects found for the transition  $E-E'$ . This transition, therefore, is most likely of first order. Although the experimental evidence is not conclusive, one may speculate that the structure for  $E'$  is that of heavy or superheavy DW's in a hexagonal network.

## C. Phase transition of the light domain walls

For the *light* DW's a totally different kind of phase transition is observed. The spot profiles shown in Fig. 7 were measured at  $\theta = 0.45$ , corresponding to an average DW distance  $l$  of  $12.7 \text{ \AA}$  ( $\varepsilon = 0.098 \pm 0.005$ ). Here, the inflection point of the peak intensity, located at  $(470 \pm 5) \text{ K}$ , does not characterize the phase transition because, as illustrated in Fig. 7, a continuous shift of the peak towards higher values of  $\varepsilon$  is found for  $T > 470 \text{ K}$ . At the same time a second, much broader peak (II) evolves on the left side of this first peak (I). Peak (II) also shifts continuously to higher values of  $\varepsilon$  with temperature. Its intensity increases relative to that of peak (I), and at  $T \sim 660 \text{ K}$  peak (I) finally vanishes. The positions of the two peak maxima as a function of  $T$  are shown in Fig. 8. The FWHM of peak (I) remains approximately constant up to  $\sim 560 \text{ K}$  and increases at higher  $T$  until the peak disappears. This spot profile evolution is observed for two of the six satellites indexed as No. 3 in the diffraction pattern of Fig. 2. The other four satellites vanish with the same temperature dependence as peak (I), but no additional peaks can be detected close to their position. From the different diffraction patterns below and above

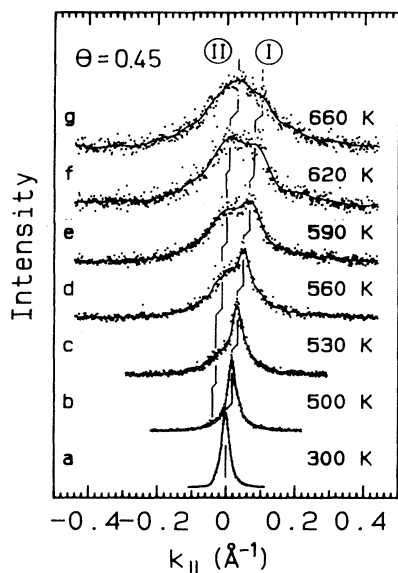


FIG. 7. Phase transition of the light DW's ( $E$ ) to the disordered lattice gas at  $\theta = 0.45$ . Diffraction profiles perpendicular to the DW's as a function of temperature (spot No. 3; see Fig. 2). The zero position of the  $k_{\parallel}$  axis is fixed to the position of the spot at low temperatures. The solid lines serve as guidelines for the eye.

the phase transition it is obvious that the high- and low-temperature phases have different structures. As peak (II) is very broad, the high-temperature phase must be strongly disordered, and only short-range-order correlations of 45 Å at most remain. The diffraction pattern of the disordered phase can be best described as an incommensurate hexagonal structure, which is rotated with respect to the substrate lattice. A matrix notation can be

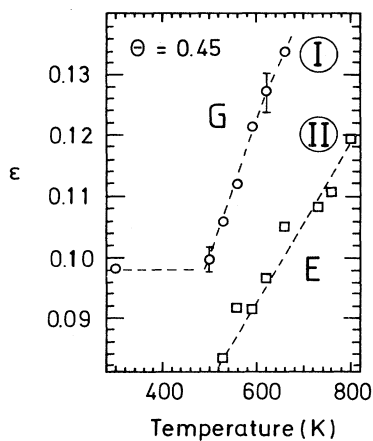


FIG. 8. Peak positions as a function of temperature for the light DW phase  $E$  ( $\circ$ ) and the incommensurate phase ( $\square$ ). Positions are measured in units of  $a^*$  with respect to the position of the commensurate  $(\sqrt{3} \times \sqrt{3})R30^\circ$  superstructure spot.

given as  $\begin{pmatrix} 1/3-1/\sqrt{3}\epsilon, & 1/3+2/\sqrt{3}\epsilon \\ -1/3-2/\sqrt{3}\epsilon, & 2/3+1/\sqrt{3}\epsilon \end{pmatrix}$ , where the parameter  $\epsilon$  depends on temperature.

As a function of  $T$ , the evolution of the spot profiles indicates a transition from the ordered DW phase at low temperatures to a short-range-ordered phase by crossing an intermediate *coexistence region* in which domains of both phases are present on the surface. Assuming no reentrant topology of the phase diagram,<sup>11</sup> and the relation between coverage and spot splitting given by Eq. (1) still to be valid at these elevated temperatures, we can draw plausible phase boundaries of this coexistence region, although the density of the short-range-ordered phase is not known precisely. These results are drawn in Fig. 9 together with the data from previous measurements. The boundary lines at coverages  $\Theta > 0.42$  shown there mark first-order phase transitions with a liquidus and a solidus line analogous to phase diagrams in three dimensions. The peak shifts may be indicative for temperature-dependent changes of local coverage (see Fig. 9).

At present, no conclusive structural model for the disordered phase can be given. At first sight, obvious candidates for structural models seem to be DW structures with lower local densities of atoms in the DW's (with respect to the ordered DW phase at low  $T$ ), e.g., the DW models (b) and (c) of Fig. 4, and much stronger fluctuations in the DW distance. However, these models would lead to different diffraction patterns than observed at high temperature. On the other hand, this phase is definitely not a homogeneous hexagonal incommensurate phase. This type of phase, although compatible with the LEED pattern, would have a significantly too small coverage.

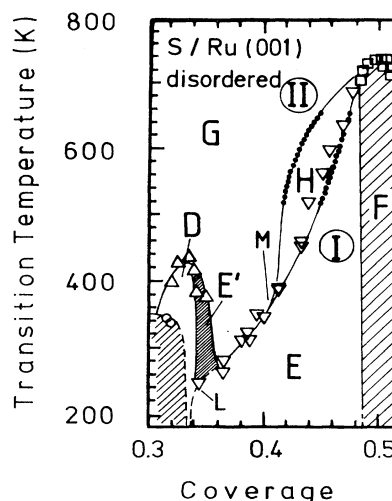


FIG. 9. Section of the phase diagram of S/Ru(0001) for coverages between 0.30 and 0.52. Open symbols are measurements from Ref. 24.  $D$ ,  $(\sqrt{3} \times \sqrt{3})R30^\circ$ ;  $E'$ ,  $(\sqrt{3} \times \sqrt{3})R30^\circ$  with line defects;  $E$ , striped network of domain walls;  $F$ ,  $c(2 \times 4)-2S$ ;  $G$ , disordered phase;  $H$ , coexistence region.  $M$  and  $L$  denote multicritical points. Small dots mark the coexistence region  $H$ , as far as measured.

#### D. Phase transition of the $c(2 \times 4)$ phase

At completion of the  $c(2 \times 4)$  structure at a coverage of 0.50 the phase boundary has a maximum (see Fig. 9). As a consequence of this topology, no coexistence region can exist between the ordered  $c(2 \times 4)$  and the disordered phase at  $\theta = 0.50$  (see Ref. 42) so that the transition must proceed directly from the ordered  $c(2 \times 4)$  phase to the disordered phase also for a first-order phase transition.

The spot profiles of the ordered  $c(2 \times 4)$  phase are instrument limited, indicating the existence of long-range  $c(2 \times 4)$ -ordered domains of at least  $\sim 400$  Å in diameter. The disordered phase at high  $T$  still contains short-range correlations and leads to a diffraction pattern with broad peaks similar to that observed for the disordered phase at  $\theta = 0.45$ , except that  $\varepsilon = 1/(4\sqrt{3})$  at  $\theta = 0.5$ . We note that no peak shifts are found at this coverage.

At the phase transition a sharp decrease of the intensities of all superstructure spots is observed, and the  $I(T)$  curves drop to the background level within only  $\sim 7$  K above the inflection points. The transition temperature as determined from the inflection points of all measured beams is identical ( $745 \pm 0.5$  K). Above the inflection point a sharp increase of the FWHM is observed. This behavior is illustrated in Fig. 10 for the  $(1/2, 1/4)$  superstructure spot, which corresponds to spot No. 2 of the DW diffraction pattern (see Fig. 3). As there is no intensity contribution from the disordered phase at this spot position, this spot is suited for analysis of the decay of the  $c(2 \times 4)$  order.

In order to reveal the nature of this  $c(2 \times 4)$  phase transition, we analyzed the profiles of the  $(1/2, 1/4)$  spot as a function of temperature using the same data evaluation as for the continuous DW transition at  $\theta = 0.40$ . The scan direction was chosen to minimize the FWHM of the profile at low  $T$  by scanning parallel to the direction of the preferentially oriented steps of the surface.<sup>43</sup> The parametrization of Eq. (2) was used for fitting the profiles, with  $\eta$  set to zero and  $\xi_{\parallel} = \xi_{\perp}$ . Although the profiles are slightly asymmetric, no systematic deviations of the fits were found. Fitted values of  $\xi$  are plotted versus the reduced temperature in Fig. 11. Again,  $T_c$  was set to the inflection point of the  $I(T)$  curve. As seen from Fig. 11, the observed temperature behavior of  $\xi$  is compatible with a power law behavior [Eq. (4)]. However,

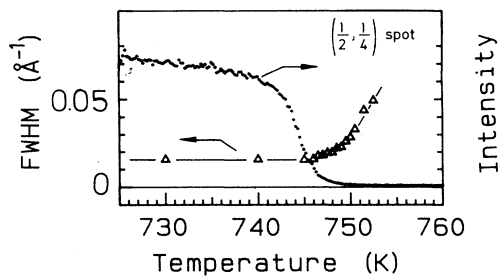


FIG. 10. Phase transition of the  $c(2 \times 4)$  structure ( $\theta = 0.50$ ). Peak intensity and FWHM of the  $(1/2, 1/4)$  spot versus temperature.

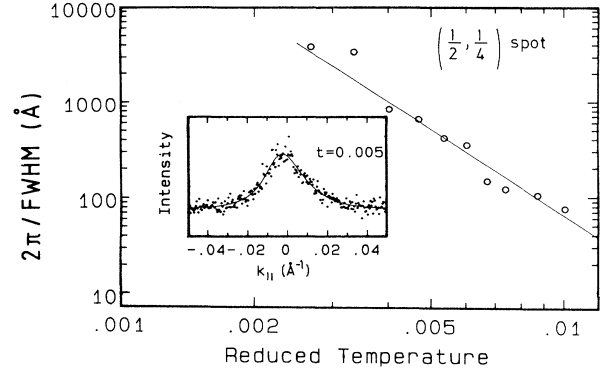


FIG. 11.  $c(2 \times 4)$  phase transition. Fitted inverse FWHM versus reduced temperature above the phase transition. The line is fit to a power law  $t^{-\nu}$  with  $\nu = 3.0$ . The inset shows a typical spot profile and a fit with a Lorentzian function.

the exponent  $\nu$  resulting from this evaluation is  $3 \pm 1$ . This value clearly rules out a continuous phase transition, since the scaling laws for the critical exponents limit  $\nu$  to an upper value of 1.<sup>44</sup> In addition, for continuous phase transitions critical scattering is normally present in a temperature range up to 10–30% in  $t$ , whereas here the spot broadening extends only up to  $t = 1\%$ . Therefore, the phase transition of the  $c(2 \times 4)$  structure must be of first order. This finding is in agreement with the first Landau rule.<sup>5</sup> As a consequence, the fitted inverse half widths have to be interpreted as average sizes of ordered domains at the phase transition. The simultaneous presence of both  $c(2 \times 4)$ -ordered and disordered regions in a finite-temperature range around the transition temperature, as found here, is a consequence of the inhomogeneity of the system due to finite-size effects,<sup>45</sup> i.e., due to terraces on the surface. Therefore, the broadening of profiles cannot be related to a correlation length of critical fluctuations in this case.

#### V. DISCUSSION

For the two different types of DW's and the  $c(2 \times 4)$  structure of S/Ru(0001) we find three different types of temperature-induced order-disorder phase transitions. For the superheavy walls, which are present at low coverages, the observation of a *continuous* transition agrees with the theoretical prediction for striped DW's in a  $\sqrt{3}$  structure on the basis of the free fermion model.<sup>11</sup> This indicates that the DW model, which was mainly developed for the limit of large DW distances in weakly bound physisorbed systems, seems to be still applicable for the situation of rather small DW distances (as here) in chemisorbed systems. As we showed, the evolution of the spot profiles is compatible with the formation of free dislocations in the DW network, which are the basic excitations of a KT transition. The observed increase of the exponent  $\eta$  with  $T$  also agrees with this type of transition, whereas it should be constant at continuous phase transitions with power law singularities (e.g., tran-



sitions in the Potts universality classes). However, a new mechanism of creating additional wall length seems to be effective in the system investigated here, leaving the average distance between walls unchanged as a function of temperature. A possible mechanism would be the creation of point defects. As the creation of these defects within the walls would destabilize them, and also for entropic reasons, the creation of point defects within the  $\sqrt{3}$  domains is more probable.

The difficulty to uniquely distinguish between power law singularities and a KT transition is not limited to our experiment. The same problem has been found in earlier experiments as well with considerably better overall resolution than here (see, e.g., the analysis of melting of Ar on graphite by Nielsen *et al.*<sup>39</sup>). For a discrimination of the two types of transitions, data over a much wider temperature range would be needed, but limits are set by finite-size effects due to monoatomic steps in our experiment.<sup>8</sup>

An increase of coverage not only causes a transformation from a superheavy DW structure with  $\sqrt{3}$  ordered domains to light DW's with  $c(2 \times 4)$ -ordered domains, but we find also a direct correlation of this structural change with the occurrence of a first-order phase transition in the light DW structure. One reason for the change to a first-order transition might be that a grain-boundary-induced melting<sup>17</sup> (of first order) becomes energetically more favorable with respect to the excitation of free dislocations in the DW network at high coverages. This change of mechanism leading to a phase transition might in turn be caused by a coverage-dependent modification of lateral interactions. Indeed, MC simulations with a constant set of interactions could not reproduce the strong increase of transition temperatures close to the coverage of 0.5.<sup>31</sup> On the other hand, considering just symmetry arguments, which predict a first-order phase transition for the  $c(2 \times 4)$  structure,<sup>5</sup> it might not be surprising that a diluted  $c(2 \times 4)$  structure still shows the same kind of transition. With the well-correlated defects in this case, this is still a nontrivial result.

In the range of small excess coverages above 0.33, i.e., in the low-concentration limit of domain walls, the S/Ru(0001) phase diagram is most directly comparable to existing theories. It is clear from our experiment that both in  $E$  and  $E'$  phases line defects exist. Although details cannot be resolved here, we would like to shortly sketch the possible explanations for our findings. The transition line between the commensurate  $\sqrt{3}$  structure and a striped DW phase is expected to be a continuous transition.<sup>15</sup> Our experimental data at low  $T$  ( $\theta = 0.34$ – $0.35$ ,  $T_c \leq 240$  K) are indeed compatible with a continuous transition, i.e., with the scenario that the DW distance gets very large when the transition line is approached from higher coverages. As mentioned, the profile broadening, which discriminates the  $E'$  phase from the commensurate  $\sqrt{3}$  phase, indicates that line defects are also present in the  $E'$  phase. Villain has shown that at low coverages a DW phase with a hexagonal DW network may be favored at higher temperature over a DW phase with a striped network even in the case of repulsive wall crossing energy, because of the breathing en-

ergy that might overcompensate the positive energy of the wall crossings.<sup>46</sup> Therefore, the  $E'$  phase is a candidate for a hexagonal network of superheavy domains. The hysteresis found in our experiments going from the  $E$  to the  $E'$  phase can be taken as an indication for a first-order phase transition, which is expected for a transition from striped to hexagonal domain walls. If, on the other hand, the activation of point defects is important also at low wall concentrations, a continuous depinning phase transition<sup>15</sup> can also occur, leaving the striped domain wall phase intact.<sup>47</sup> In this case the observed hysteresis might simply be due to slow kinetics in this activated process.

With increase of coverage, the transition between the striped DW phases ( $E$ ) and the disordered phase changes from a continuous to a first-order-type transition. As a consequence there must be a multicritical point ( $M$  in Fig. 9) at  $\theta \simeq 0.42$  and  $T_c \simeq 360$  K, where the continuous transition line splits into the two first-order transition lines (solidus and liquidus), which limit the coexistence region of the DW phase and the disordered phase. Another multicritical point must be present ( $L$  in Fig. 9), which is the point where the Pokrovskii-Talapov (PT) and KT transition lines merge, a so-called Lifschitz point.<sup>11</sup> Under the condition that the transition from the  $\sqrt{3}$  phase to the DW phase and the transition from the DW phase to the disordered phase are of PT and KT type, the Lifschitz point would be located at  $\theta \simeq 0.35$  and  $T_c \simeq 240$  K in this system (see Fig. 9).

From our profile analysis, the order-disorder phase transition of the  $c(2 \times 4)$  structure is clearly shown to be of first order. This result is in agreement with the first Landau rule, which does not allow a continuous phase transition for this superstructure.<sup>5</sup> As a consequence of finite-size effects, the intensity does not disappear abruptly at the transition.<sup>45</sup> Instead,  $c(2 \times 4)$ -ordered domains of decreasing size exist over a small range in reduced temperature of  $\sim 1\%$ . It is very likely that these finite-size effects are due to the monoatomic steps on this surface. For the continuous  $p(2 \times 2)$  and  $\sqrt{3}$  phase transitions, we found earlier that the steps cause a finite-size rounding over approximately the same range in reduced temperature.<sup>8</sup> For a first-order phase transition, a finite-size rounding of the transition proportional to  $L^{-D}$  ( $L$  being the system size) is expected. A more detailed study of the influence of steps on the  $c(2 \times 4)$  phase transition, using vicinal surfaces of different step density, could test this prediction. This study, however, would be complicated by the fact that S causes changes in the surface morphology by step bunching at these coverages and at elevated temperatures.<sup>8</sup>

## VI. CONCLUSIONS

Our results show that temperature-induced DW phase transitions of an atomic chemisorbate are well suited to study experimentally the phase transitions of striped DW's. First-order as well as continuous phase transitions of various kinds could be identified. The variety of phase transitions observed is comparable to those of physisorbed systems, but chemisorbed systems are more easily accessible. Our experiments show that a

Kosterlitz-Thouless type of phase transition seems to occur even up to wall densities of only a few lattice constants. An interesting modification, however, was found, leaving the average wall distance constant throughout the phase transition. No conclusive mechanism for this finding has yet been proposed.

## ACKNOWLEDGMENTS

We are indebted to R. Dennert for contributions in earlier discussions. This work has been supported by the Deutsche Forschungsgemeinschaft.

- \* Current address: Physikalisches Institut der Universität Würzburg EPII, Am Hubland, D-97074 Würzburg, Germany; FAX: +49-931-888-5158.
- † FAX: +49-511-762-4877; electronic address: pfnuer@dynamic.fkp.uni-hannover.de
- <sup>1</sup> E. Bauer, in *Structure and Dynamics of Surfaces II*, edited by W. Schommers and P. von Blanckenhagen (Springer, New York, 1987), Vol. 43, p. 115.
  - <sup>2</sup> T. L. Einstein, in *Proceedings of the 10th John Hopkins Workshop*, edited by K. Dietz and V. Rittenberg (World Scientific, Singapore, 1987), p. 17.
  - <sup>3</sup> W. N. Unertl, *Comments Condens. Matter. Phys.* **12**, 289 (1986).
  - <sup>4</sup> B. N. J. Persson, *Surf. Sci. Rep.* **15**, 1 (1992).
  - <sup>5</sup> M. Schick, *Prog. Surf. Sci.* **11**, 245 (1981).
  - <sup>6</sup> K. Binder and D. P. Landau, in *Molecule-Surface Interaction*, edited by K. Lawley (Wiley, New York, 1989), p. 91.
  - <sup>7</sup> P. Piercy and H. Pfnür, *Phys. Rev. Lett.* **59**, 1124 (1987); H. Pfnür and P. Piercy, *Phys. Rev. B* **40**, 2515 (1989).
  - <sup>8</sup> M. Sokolowski and H. Pfnür, *Phys. Rev. B* **49**, 7716 (1994).
  - <sup>9</sup> M. Sokolowski and H. Pfnür, *Phys. Rev. Lett.* **63**, 183 (1989).
  - <sup>10</sup> L. Schwenger, K. Budde, C. Voges, and H. Pfnür, *Phys. Rev. Lett.* **73**, 296 (1994).
  - <sup>11</sup> M. den Nijs, in *Phase Transitions and Critical Phenomena*, edited by C. Domb and J. L. Lebowitz (Academic Press, New York, 1988), Vol. 12, p. 219.
  - <sup>12</sup> C. Schwennicke, D. Jürgens, G. Held, and H. Pfnür, *Surf. Sci.* **316**, 87 (1994).
  - <sup>13</sup> D. Jürgens and H. Pfnür (unpublished).
  - <sup>14</sup> K. J. Strandburg, *Rev. Mod. Phys.* **60**, 161 (1988).
  - <sup>15</sup> V. L. Pokrovskii and A. L. Talapov, *Sov. Phys. JETP* **51**, 134 (1980).
  - <sup>16</sup> S. N. Coppersmith, D. S. Fisher, B. I. Halperin, P. A. Lee, and W. F. Brinkman, *Phys. Rev. B* **25**, 349 (1982).
  - <sup>17</sup> S. T. Chui, *Phys. Rev. Lett.* **48**, 933 (1982); *Phys. Rev. B* **28**, 178 (1983).
  - <sup>18</sup> R. Imbühl, R. J. Behm, K. Christmann, G. Ertl, and T. Matsushima, *Surf. Sci.* **117**, 257 (1982).
  - <sup>19</sup> B. N. J. Persson, *Appl. Phys. A* **51**, 91 (1990).
  - <sup>20</sup> R. Schuster, J. V. Barth, G. Ertl, and R. J. Behm, *Phys. Rev. Lett.* **69**, 2547 (1992).
  - <sup>21</sup> K. Kern, in *Chemistry and Physics of Solid Surfaces VII*, edited by R. Vanselow and R. F. Howe (Springer-Verlag, Berlin, 1988), p. 455.
  - <sup>22</sup> J. Cui and S. C. Fain, Jr., *Phys. Rev. B* **39**, 8628 (1989).
  - <sup>23</sup> R. Diehl and S. C. Fain, Jr., *Surf. Sci.* **125**, 116 (1983).
  - <sup>24</sup> R. Dennert, M. Sokolowski, and H. Pfnür, *Surf. Sci.* **271**, 1 (1992).
  - <sup>25</sup> D. Jürgens, G. Held, and H. Pfnür, *Surf. Sci.* **303**, 77 (1994).
  - <sup>26</sup> D. Heuer, T. Müller, H. Pfnür, and U. Köhler, *Surf. Sci. Lett.* **297**, L61 (1993).
  - <sup>27</sup> T. Müller, D. Heuer, U. Köhler, and H. Pfnür, *Surf. Sci.* (to be published).
  - <sup>28</sup> W. Sklarek, C. Schwennicke, D. Jürgens, and H. Pfnür, *Surf. Sci.* (to be published).
  - <sup>29</sup> C. Schwennicke, M. Sandhoff, W. Sklarek, D. Jürgens, and H. Pfnür, *Phys. Rev. B* (to be published).
  - <sup>30</sup> M. Sandhoff, H. Pfnür, and H.-U. Everts, *Europhys. Lett.* **25**, 105 (1994).
  - <sup>31</sup> M. Sandhoff, H. Pfnür, and H.-U. Everts (unpublished).
  - <sup>32</sup> N. C. Bartelt, T. L. Einstein, and L. D. Roelofs, *Phys. Rev. B* **32**, 2993 (1985).
  - <sup>33</sup> H. Schlichting and D. Menzel, *Surf. Sci.* **285**, 209 (1993).
  - <sup>34</sup> U. Scheithauer, G. Meyer, and M. Henzler, *Surf. Sci.* **178**, 441 (1986).
  - <sup>35</sup> P. Zeppenfeld, K. Kern, R. David, and G. Comsa, *Phys. Rev. B* **38**, 3918 (1988).
  - <sup>36</sup> The commensurability of 4 for the  $c(2 \times 4)$  structure is given by the primitive unit cell (see Fig. 1).
  - <sup>37</sup> M. E. Fisher, *J. Math. Phys.* **5**, 944 (1964).
  - <sup>38</sup> D. R. Nelson and B. I. Halperin, *Phys. Rev. B* **19**, 2457 (1979); A. P. Young, *ibid.* **19**, 1855 (1979).
  - <sup>39</sup> M. Nielsen, J. Als-Nielsen, J. Bohr, J. P. McTague, D. E. Moncton, and P. W. Stephens, *Phys. Rev. B* **35**, 1419 (1987).
  - <sup>40</sup> H. E. Stanley, *Phase Transitions and Critical Phenomena* (Oxford University Press, Oxford, 1971).
  - <sup>41</sup> P. Bak, in *Chemistry and Physics of Solid Surfaces VII*, edited by R. Vanselow and R. F. Howe (Springer, Berlin, 1984), p. 317.
  - <sup>42</sup> L. D. Landau and E. M. Lifschitz, *Lehrbuch der Theoretischen Physik* (Akademie-Verlag, Berlin, 1979), Vol. 5.
  - <sup>43</sup> As reported in Ref. 8 the monoatomic steps on the surface stem from a slightly vicinal orientation of the surface with respect to the (0001) plane. They are thus approximately parallel.
  - <sup>44</sup> From the scaling law  $2 - D\nu = \alpha$  ( $D$  being the dimension, i.e., 2 in our case) (Ref. 40), using a positive value for the specific heat, exponent  $\alpha$ , one deduces  $\nu \leq 1$ .
  - <sup>45</sup> K. Binder, *Prog. Phys.* **50**, 784 (1987).
  - <sup>46</sup> J. Villain, in *Ordering in Two Dimensions*, edited by S. K. Sinha (North-Holland, New York, 1980), p. 123.
  - <sup>47</sup> I. Lyuksyutov (private communication).